

DISTRIBUTED SENSING OF LOADS ACTING AGAINST THE HULL OF A STATIONKEEPING VESSEL IN ICE

Hans-Martin Heyn
Department of Marine
Technology
Norwegian University of Science
and Technology,
7491 Trondheim, Norway

Roger Skjetne
Department of Marine
Technology
Norwegian University of Science
and Technology,
7491 Trondheim, Norway

Francesco Scibilia
Statoil ASA
Arkitekt Ebbells veg 10,
7053 Ranheim, Norway

ABSTRACT

This paper introduces the concept of distributed motion sensing for stationkeeping vessels in ice infested waters. During the SKT 2017 project, conducted in February and March 2017 in the Bay of Bothnia, five inertial measurement units were installed on the vessel Magne Viking. Four of the sensor units were installed at different positions inside the hull of the vessel, which enabled the system to locally measure ice-induced vibrations in the hull of the vessel. The fifth sensor unit was installed at a central position of the vessel and served as reference sensor for measuring the acting global load on the vessel. Under stationkeeping the global load measured on the ship should be close to zero, because the environmental load is equal to the force from the stationkeeping system. However the remaining four motion sensor units in the hull also measured locally induced vibrations. The study shows that this sensor configuration allows for the detection of changes in the acting load against the vessel. This is demonstrated with motion data obtained during the stationkeeping trials on the vessel Magne Viking.

INTRODUCTION

Operations in ice add an additional risk. To ensure that the ship is operated within its safety limits, and to achieve additional class notations, classification societies recommend the measurement of ice loads acting against the vessel [1], [2].

Typically, strain gauges measure the local deformation of the hull and thus provide local load measurements [3]. An inertial measurement unit (IMU), typically located at a central position of the vessel (e.g. close to the centre of orientation (CO)), provides globally acting accelerations (and loads) [4].

The interaction with ice induces vibrations in the hull [5]. By placing IMUs closer to the ice interaction zones (i.e. the bow of the vessel), locally induced vibrations, caused by the ship-ice interaction, can be recorded and conclusions on the acting local

load drawn [6]. By placing several IMUs at different location of the vessel, a more stable estimate of the globally acting load can be obtained [7]. By using a distributed network of IMUs placed close to the ice interaction zone, and at central positions of the vessel, both locally induced accelerations and, by merging the data from all IMUs, stable global accelerations can be measured.

Distributed IMU systems were developed and tested in 2015 and 2016 on two icebreakers operating in ice [8], [9]. However, both vessel never operated in stationkeeping mode. In this study it will be investigated, if distributed motion sensing can be used to identify the intensity and direction of ice action against a stationkeeping vessel.

This is a level 3 paper in the SKT project, with the focus on describing the measurement setup for distribution ice load sensing. The project overview is given in the level 1 paper [10]. This paper presents a mathematical model for locally induced accelerations. The measurement setup will be described. A case study in which the direction of the load acting against the vessel is determined motivates further research, which will be subject of future publications.

NOMENCLATURE

The following notation is used throughout this paper:

- A subscript to a vector $\mathbf{x} \in \mathbb{R}^3$ gives reference to a coordinate reference frame.
- An acceleration vector $\mathbf{a}_{ab}^c \in \mathbb{R}^3$ represents the acceleration of frame $\{b\}$, relative to frame $\{a\}$, decomposed in frame $\{c\}$.
- An Euler angle vector $\boldsymbol{\theta} \in \mathcal{S}^3$ describing the angles from $\{a\}$ to $\{b\}$ is denoted $\boldsymbol{\theta}_{ab}$.
- A rotation matrix $\mathbf{R}_c^d \in \mathcal{SO}(3)$ transforms a vector from frame $\{c\}$ to frame $\{d\}$. This can be parameterised by an Euler angle vector, $\mathbf{R}(\boldsymbol{\theta}_{dc})$, where $\mathbf{R}(\cdot)$ is given in [11], Eq. 2.18.

- The derivation of a rotation matrix $\mathbf{R}_c^d = \mathbf{R}_c^d \mathbf{S}(\boldsymbol{\omega}_{dc}^c)$, where $\mathbf{S}(\boldsymbol{\omega}_{dc}^c)$ is skew-symmetric matrix, depending on the angular velocity vector $\boldsymbol{\omega}_{dc}^c$ and given as

$$\mathbf{S}(\boldsymbol{\omega}) = \begin{bmatrix} 0 & -\omega_z & \omega_y \\ \omega_z & 0 & -\omega_x \\ -\omega_y & \omega_x & 0 \end{bmatrix} \quad (1)$$

MATHEMATICAL MODEL OF IMU MEASUREMENTS

An IMU contains a triaxis accelerometer, which measures the specific forces $\mathbf{f}_{IMU,s}^s$, and a triaxis gyroscope, which measures the angular rates $\boldsymbol{\omega}_{IMU,s}^s$. All measurements are obtained in the sensor's coordinate frame $\{s\}$. The vector $\boldsymbol{\Theta}_{bs}$ gives the orientation angles of the sensor with respect to the body frame $\{b\}$ of the vessel. The specific force readings can be transferred to the body frame of the vessel:

$$\mathbf{f}_{IMU,s}^b = \mathbf{R}(\boldsymbol{\Theta}_{bs}) \mathbf{f}_{IMU,s}^s \quad (2)$$

It will be assumed, that readings from all IMUs are transformed to the body frame of the vessel, and thus all sensors are aligned with the ship's coordinate system, as illustrated in Figure 1. The specific force readings include the sensed acceleration of the IMU with respect to an inertial frame $\mathbf{a}_{is}^b = \mathbf{R}_i^b \ddot{\mathbf{p}}_{is}^i$, a gravitational vector $\bar{\mathbf{g}}^n$, accelerometer bias $\mathbf{b}_{a_s}^b$, and sensor noise $\boldsymbol{\omega}_{a_s}^b$ [12]:

$$\mathbf{f}_{IMU,s}^b = \mathbf{a}_{is}^b - \mathbf{R}_n^b \bar{\mathbf{g}}^n + \mathbf{b}_{a_s}^b + \boldsymbol{\omega}_{a_s}^b \quad (3)$$

Analogously the sensor output of the gyro is given as:

$$\boldsymbol{\omega}_{IMU}^b = \boldsymbol{\omega}_{ib}^b + \mathbf{b}_{\omega_s}^b + \boldsymbol{\omega}_{\omega_s}^b \quad (4)$$

To transform the sensor sensed accelerations \mathbf{a}_{is}^b to the accelerations felt at any other location b within the ship (e.g. centre of orientation (CO)), the centripetal accelerations $\mathbf{S}(\boldsymbol{\omega}_{ib}^b)^2 \mathbf{l}_s^b$ and Euler accelerations $\mathbf{S}(\boldsymbol{\alpha}_{ib}^b) \mathbf{l}_s^b$ have to be accounted for:

$$\mathbf{a}_{ib}^b = \mathbf{a}_{is}^b - \mathbf{S}(\boldsymbol{\omega}_{ib}^b)^2 \mathbf{l}_s^b - \mathbf{S}(\boldsymbol{\alpha}_{ib}^b) \mathbf{l}_s^b \quad (5)$$

The sensed acceleration $\mathbf{f}_{IMU,s}^b$ at the sensor's location contains the translational acceleration component \mathbf{a}_{is}^b , and, in addition, a local vibration component $\mathbf{a}_{vib,s}^b$ may be present. Only a sensor in close proximity to the vibration's source can sense the local vibration component, because it is typically damped out through the hull structure. Hence, a sensor close to a local vibration source (i.e. the hull during ship-ice interaction) measures the following acceleration:

$$\begin{aligned} \mathbf{a}_{ib}^b &= \mathbf{a}_{is}^b - \mathbf{S}(\boldsymbol{\omega}_{ib}^b)^2 \mathbf{l}_s^b - \mathbf{S}(\boldsymbol{\alpha}_{ib}^b) \mathbf{l}_s^b \\ &= \mathbf{f}_{IMU,s}^b + \mathbf{R}_n^b \bar{\mathbf{g}}^n - \mathbf{S}(\boldsymbol{\omega}_{ib}^b)^2 \mathbf{l}_s^b - \mathbf{S}(\boldsymbol{\alpha}_{ib}^b) \mathbf{l}_s^b \\ &\quad - \mathbf{a}_{vib,s}^b - \mathbf{b}_{a_s}^b - \boldsymbol{\omega}_{a_s}^b \end{aligned} \quad (6)$$

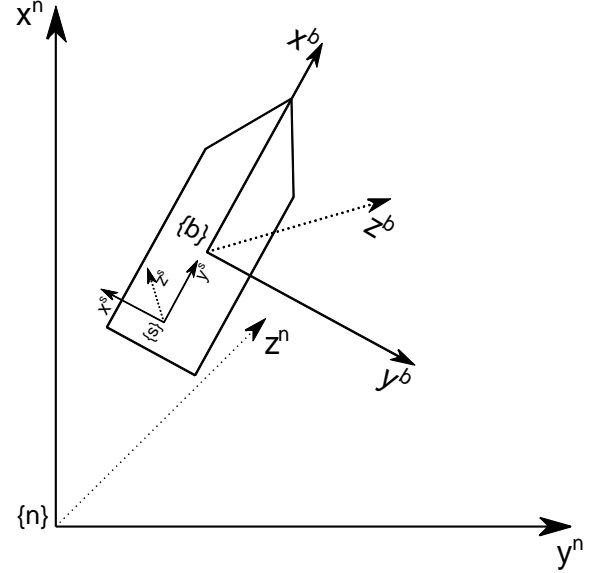


Figure 1. North-East-Down (NED) frame $\{n\}$, Sensor frame $\{s\}$ and body frame $\{b\}$ of the vessel

MEASUREMENT SETUP ON MAGNE VIKING

The ice-class anchor handling tug supply (AHTS) vessel Magne Viking was equipped with a system of five IMUs during the SKT 2017 project. A more detailed description of the project is given in [10], and the specifications of the vessel are summarised in Table 1.

The scope of the experiment was to record globally as well as locally occurring ice-load induced accelerations. The IMUs for this experiment were ADIS16364 six degrees of freedom inertial sensors from Analog Devices. Technical details can be found in [13], and the specifications of the sensor are presented in Table 2.

Placement of sensors

To allow for a spatial resolution of locally induced accelerations, the sensors had to be placed at various positions in the vessel, preferably close to the ice-interaction zone of the hull. One sensor was placed next to the motion reference unit (MRU) of the vessel in the instrument room on D-Deck and provided global accelerations and undistributed gyro rates.

Table 1. Specification of Magne Viking

Ice Class	ICE-1A DNV-GL
IMO No	9423839
Length overall	85.20 m
Beam	22.00 m
Depth to first deck	9.00 m
Deadweight	4500 mt
Main machine	2 MAK 4000kW
Aux machine	2 MAK 3000kW
Propellers	2 control. pitch, 4250 mm
Rudder	2 spade rudders
Thrusters stern	2 tunnel thrusters, 830kW each
Thrusters bow	2 tunnel thrusters, 830kW each 1 azimuth thruster, 830kW

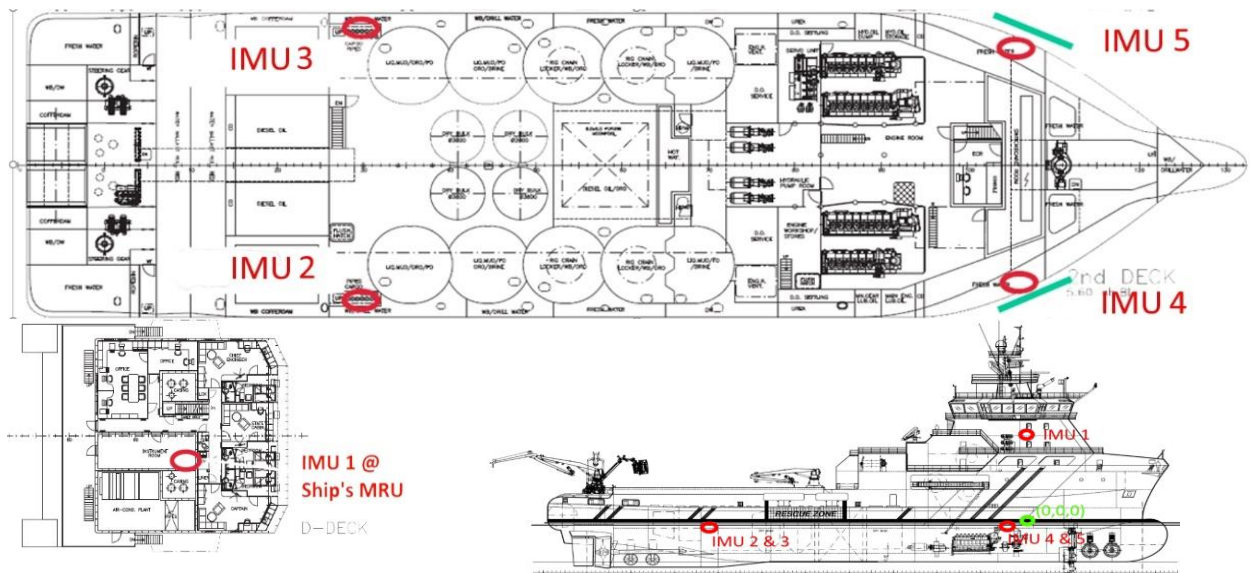


Figure 2. Placement of sensors (red: IMU sensors, green: strain gauges, top: 2nd Deck, bottom left: D-Deck, bottom right: side view)

Table 2. Technical specifications of IMUs ADIS 16364 [13]

Triaxis Accelerometer	
Dynamic range	±5.25 g
Sensitivity	1.00 mg/LSB
Bias stability	0.1 mg
Velocity random walk	012 m/s/hr ^{0.5}
Output noise	5 mg rms
Triaxis Gyro	
Dynamic range	±350 °/s
Sensitivity	0.05 °/s/LSB
Bias stability	0.007 °/s
Initial bias error	±3 °/s
Angular random walk	2.0 °/hr ^{0.5}
Output noise	0.8 °/s rms

Two sensors were placed in a tank directly on the hull in the bow of the vessel on the starboard and port side. Those two sensors were installed in the same compartment as the strain gauges measurements (see [14]). The purpose is to allow for comparison between the loads measured from the strain gauges and the results from the IMU measurements at those two positions. Further sensors were placed starboard and port in the aft of the vessel.

Orientation of sensors

Out of practical considerations, the sensors could not be placed aligned with the ship's coordinate system. Instead, each sensor had to be placed with an individual orientation, as it is illustrated in Figure 1. Table 3 contains the position of the sensors, in reference to an origin located at x-position of the IMU 1 sensor, midship as y-coordinate origin, and at nominal water level as z-coordinate origin. As coordinate system, the ahead-starboard-down system, as illustrated in Figure 1 is used. The

Euler angles in Table 3 are the components of the orientation vector θ_{bs} , where $\{b\}$ is the ship's body frame and $\{s\}$ the individual sensor's coordinate system.

Table 3. Positions and orientations of IMU sensors

IMU Place	l_s^b			θ_{bs}		
	x	y	z	ϕ	θ	ψ
1 Ship's MRU	0.00 m	2.33 m	-14.90 m	180.60°	-1.20°	0.00°
2 Aft starboard	-41.88 m	9.89 m	1.50 m	180.55°	1.00°	90.00°
3 Aft port	-41.88 m	-9.89 m	1.00 m	179.45°	-1.30°	-90.00°
4 Bow starboard	-2.33 m	8.73 m	1.00 m	179.80°	0.00°	90.00°
5 Bow port	-2.33 m	-8.73 m	1.00 m	179.20°	0.18°	-90.00°

Data collection and synchronisation of sensors

A central server collected the data from the individual IMU sensors. All data was stored on a network-attached storage to ensure file safety and backup. A detailed signal flow plan is given in the Appendix. Each IMU is controlled by a Beaglebone embedded computer. Upon initialisation, the algorithm in the central computer first requested a synchronisation of the internal real-time clocks (RTC) of the sensor units' Beaglebone computers with the ship's GPS synchronised clock. After all clocks were synchronised with the ship's time, the measurements of all five sensors started simultaneously at a set time. The data from the IMUs were recorded with a sampling rate of 300-Hz. During the measurements, the data of each unit were stored internally on a SD-card in the Beaglebone minicomputer. Upon completion of the measurement, the collected data were transferred to the network-attached storage.

PROCESSING OF IMU DATA

The raw data collected from the sensors need to be processed before the collected data can be used. The processing steps are similar to what has been described in [9] and will be explained step by step. Figure 3 gives an overview of the processing steps.

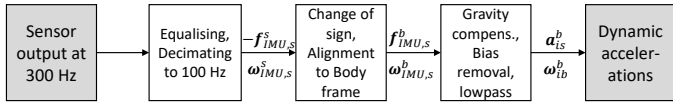


Figure 3. Processing steps of IMU data

1. The measurements were taken with a sampling rate of 300~Hz.
2. In a first step, the data from all IMUs is equalised and decimated (i.e. lowpass filtered and resampled) to 100~Hz.
3. The IMUs follow an ahead-right-down coordinate system, as defined in Figure 1. However, the accelerometer produce a positive output in the opposite direction of the axes. This is illustrated in Figure 4. Furthermore, the measurements are rotated to the ship's body frame, using equation (2). The orientation angles given in Table 3 describe the rotation from body frame to the sensor frame. To rotate the sensor readings to the body frame, three principal rotations about the z, y and x axes are executed [11]:

$$\mathbf{R}(\Theta_{bs}) = \mathbf{R}_{z,\psi} \mathbf{R}_{y,\theta} \mathbf{R}_{x,\phi} \quad (7)$$

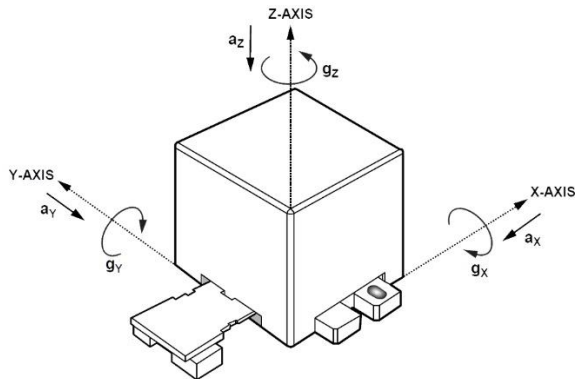


Figure 4. Coordinate system of sensor, and direction of rotation and motion (marked by arrows) that produces a positive output [13]

4. The gravity is measured by the accelerometers and needs to be removed from the readings. Furthermore, especially the gyro readings are affected by a constant bias, which needs to be removed. The effect of noise can be removed with a lowpass filter (e.g. with a cut-off frequency at 10~Hz).
5. As a result, the physical accelerations of the hull segment at the sensor's coordinates, and the angular rates of the vessel, both described in the body frame of the vessel, are obtained.

EXAMPLE STUDY

In this section, an example will be present which demonstrates the IMU's capability of recording accelerations acting against the vessel. During position mooring in managed ice, the ship moved slowly forward, until the mooring line stiffed



Figure 5. Ice conditions during position mooring on 15.03.2017 14:30 - 15:10

and kept the vessel on position. The ice was about 0.5~m thick and the ice conditions are shown in Figure 5.

Position and heading of vessel, ice drift direction, and anchor force

Figure 6 shows the GPS coordinates and the heading of the vessel over, and Figure 7 presents the propeller force. The longitudinal position changed as long as the ship moved forward, and was constant when the mooring line counteracted the motion of the vessel. The heading changed slightly from 268° to 270°.

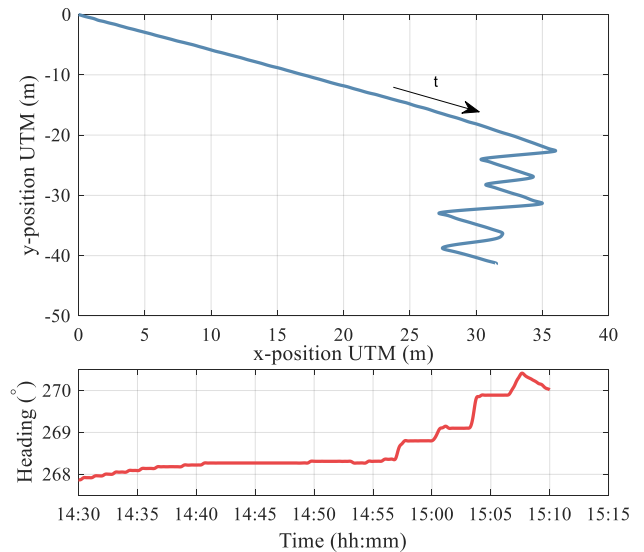


Figure 6. Position and heading of vessel over time

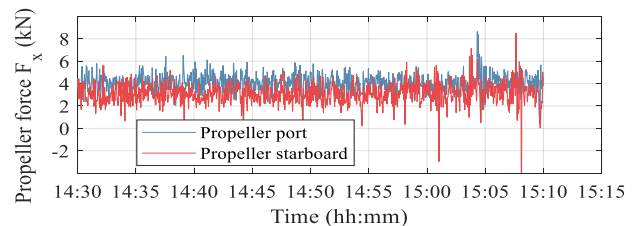


Figure 7. Force of propellers

The ice drift was measured with buoys on the ice around the stationkeeping vessel. Figure 8 shows the ice drift direction, which fluctuated between 100° and 150° degrees. The ice drift velocity was 0.02 ms⁻¹.

The anchor line was installed at the bow of the vessel, as shown in Figure 5. While the ship moved away from the anchor point, the tension in the anchor line increased. The increase in tension in the anchor line is clearly visible by the exponential increase in force in Figure 9. Once the maximum anchor force was reached, the ship experienced an acceleration in the opposite direction, forcing the vessel onto the mooring position.

IMU measurements and rotation to NED frame

The processed IMU accelerations are given in the body frame of the vessel. To allow a comparison to the acting forces against the vessel, the acceleration have to be rotated to the world north-east-down (NED) frame. Assuming that roll and pitch are small, only the yaw rotation of the vessel is relevant for the rotation:

$$\mathbf{a}_{is}^n = \mathbf{R}_{z,\psi_{ship}} \mathbf{a}_{is}^b \quad (8)$$

The yaw rotation of the vessel is given by the heading of the vessel. The heave acceleration is neglected, and only the in-plane accelerations $\bar{\mathbf{a}}_{is}^n = [a_{is,x}^n, a_{is,y}^n]^T$ are used. In order to be able to compare the measured accelerations with environmental forces, the acceleration vector $\bar{\mathbf{a}}_{is}^n$ is transformed to polar coordinates, which gives an amplitude of the acceleration \hat{a}_{is}^n and an angle $\gamma_{a_{is}^n}^n$, describing the direction the acceleration

$$\hat{a}_{is}^n = \sqrt{a_{is,x}^n{}^2 + a_{is,y}^n{}^2} \quad (9)$$

$$\gamma_{a_{is}^n}^n = \text{atan2}(a_{is,y}^n, a_{is,x}^n), \quad (10)$$

where $\text{atan2}(y,x)$ is a multi-sector inverse tangent function, which returns the angle between a vector and the origin expressed in an interval $\gamma \in (-\pi, \pi]$, which was mapped to the interval $(0^\circ, 360^\circ]$, see [11]. The transformed acceleration data from all five IMUs is plotted in Figure 10.

The plots show, that a change of direction in the measured acceleration can be detected, no matter where the IMU is installed. Some of the vibrations recorded by IMUs 2-5 might origin from the engines, but parts of the vibrations might originate from hull-ice interaction.

Further ideas for analysis

Further analysis will remove the influence of the engine noise and find the vibration components, which originate from the interaction with the sea-ice. Depending on the ice drift direction, the interaction of sea-ice with the ship's hull will occur only on some parts of the hull (e.g. only port side), and only the IMUs close to that area will measure the additional vibration component. That will give an indication of the ice drift direction around the vessel.

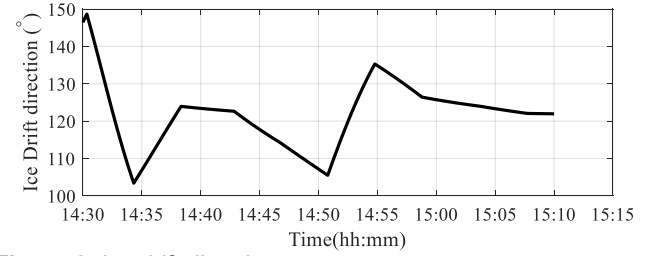


Figure 8. Ice drift direction

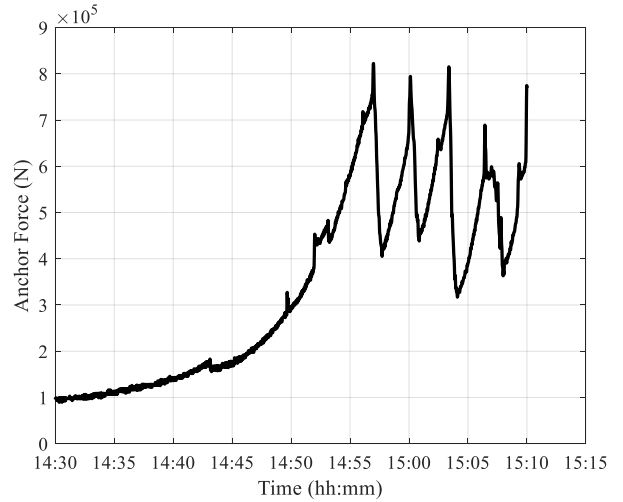


Figure 9. Anchor force

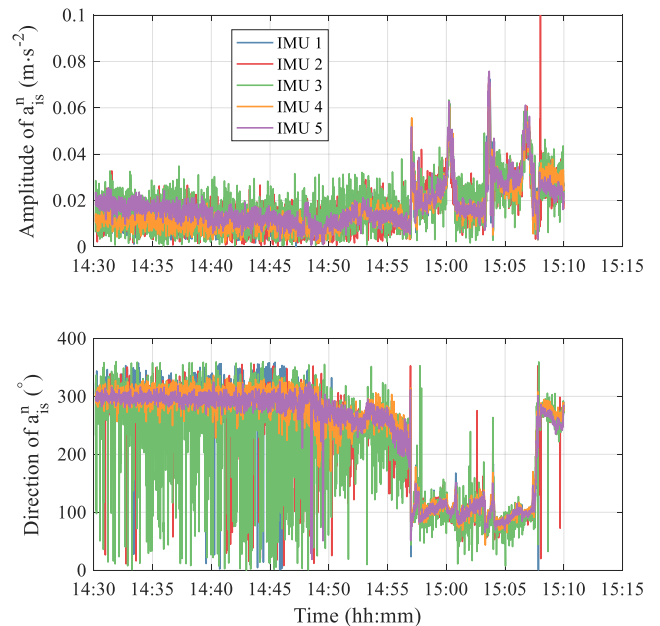


Figure 10. Amplitude and direction of measured a_{is}^n

Discussion of results

As long as the ship moved forward, the measured acceleration vector of all five IMUs pointed into the direction of travel. When the mooring line restricted the vessel's movement, the measured accelerations turns by 180°, preventing the vessel from moving further and keeping the vessel on position. This is illustrated in a polar plot in Figure 11.

Between 14:50 and 14:57, just before the anchor line reached its maximum tension, the ship was still moving forward, but the direction of the measured acceleration vector already drifted slowly from 300° to 200° because of the increased anchor force.

It is further noticeable, that the anchor line caused several spikes in the measured accelerations, which were translated into a rotational movement of the vessel, and thus a slight change of heading.

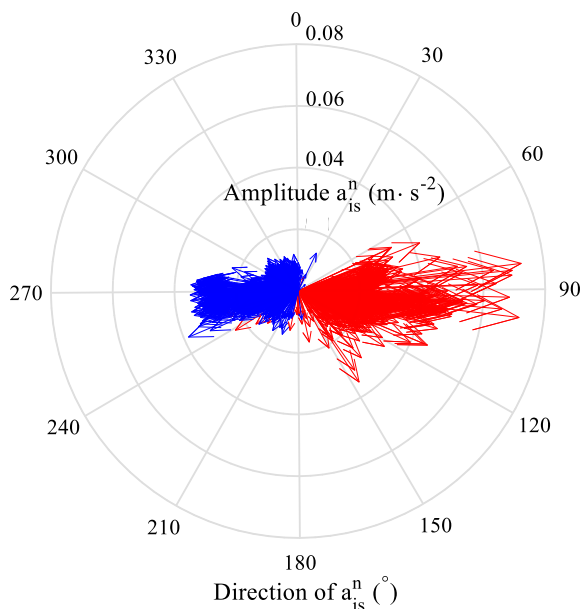


Figure 11. Polar plot of measured acceleration at IMU 1, where blue is the accelerations under forward motion and red the accelerations, when the mooring line is restricting motion of the vessel.

The shown example does not yet show any influence by the ice around the vessel. However, it shows that the sensors are sensitive to changes in the accelerations acting against the vessel and it should be possible to utilise this for detecting changes in the ice drift and ice induced acceleration amplitude around the vessel. Early detection of ice drift changes and proactive control of stationkeeping in ice using precise motion measurements will be the subject of further research using the data collected with the described sensor setup during stationkeeping in the SKT 2017 project.

Conclusion

This paper introduced a distributed inertial sensing system. A mathematical model showed, that locally measured translational accelerations include a position depending vibration component. The locally measured accelerations were mapped onto a central point in the body frame of the vessel. The main focus of this paper was to describe the measurement setup during SKT 2017 on the supply vessel Magne Viking. In an example, it was demonstrated that the sensor are capable of measuring the acting global acceleration, independent of their location within the vessel. Further studies will show that the ice induced local acceleration allow for an early detection of properties of the surrounding sea-ice, such as the ice drift direction.

ACKNOWLEDGMENTS

The authors would like to thank the Research Council of Norway (RCN) for financial support through projects 203471 CRI SAMCoT and 223254 CoE AMOS. Support to this project was provided by Statoil ASA and Statoil Greenland AS.

REFERENCES

- [1] Bureau Vertias, 'Ice Load Monitoring System', Neuilly sur Seine Cedex, 2015.
- [2] American Bureau of Shipping, 'Guide for ice loads monitoring systems', Houston, 2011.
- [3] Det Norske Veritas, *Rules for classification of ships*. Høvik, 2003, pp. 264–264.
- [4] M. Johnston, R. Frederking, G. Timco, and M. Miles, 'Using Motan To Measure Global Accelerations of the Ccgs Terry Fox During Bergy Bit Trials', *Int. Conf. Offshore Mech. Arct. Eng.*, pp. 1–8, 2004.
- [5] I. M. Belov and N. N. Spiridonov, 'Features of Ship Vibration in Ice Operation Conditions', *Twenty-second Int. Offshore Polar Eng. Conf.*, vol. 4, pp. 1223–1228, 2012.
- [6] J. Matusiak, 'Dynamic loads and response of icebreaker Sisu during continuous icebreaking', Helsinki, 1982.
- [7] O. K. Kjerstad and R. Skjetne, 'Disturbance Rejection by Acceleration Feedforward for Marine Surface Vessels', *IEEE Access*, vol. 4, pp. 2656–2669, 2016.
- [8] H.-M. Heyn and R. Skjetne, 'A System for Measuring Ice-Induced Accelerations and Identifying Ice Actions on the CCGS Amundsen and a Swedish Atle-Class Icebreaker', in *Volume 8: Polar and Arctic Sciences and Technology; Petroleum Technology*, 2016, p. V008T07A025.
- [9] H. Heyn, G. Udjus, and R. Skjetne, 'Distributed motion sensing on ships', in *Oceans 17 Conference*, 2017.
- [10] P. Liferov, 'Station-keeping trials in ice: Project Overview', in *Proceedings of the 37th International Conference on Ocean, Offshore & Arctic Engineering*, 2018.
- [11] T. I. Fossen, *Handbook of Marine Craft Hydrodynamics and Motion Control*. Chichester, UK: John Wiley & Sons, Ltd, 2011.
- [12] A. Noureldin, T. B. Karamat, and J. Georgy,

Fundamentals of inertial navigation, satellite-based positioning and their integration. Berlin, Heidelberg: Springer Berlin Heidelberg, 2013.

[13] Analog Devices Inc., 'Data Sheet ADIS 16364', Norwood, 2011.

[14] Nyseth, 'Station-keeping trials in ice: Ice load measurement system', in *Proceedings of the 37th International Conference on Ocean, Offshore & Arctic Engineering2*, 2018.

ANNEX A

NETWORK STRUCTURE OF SENSOR SYSTEM

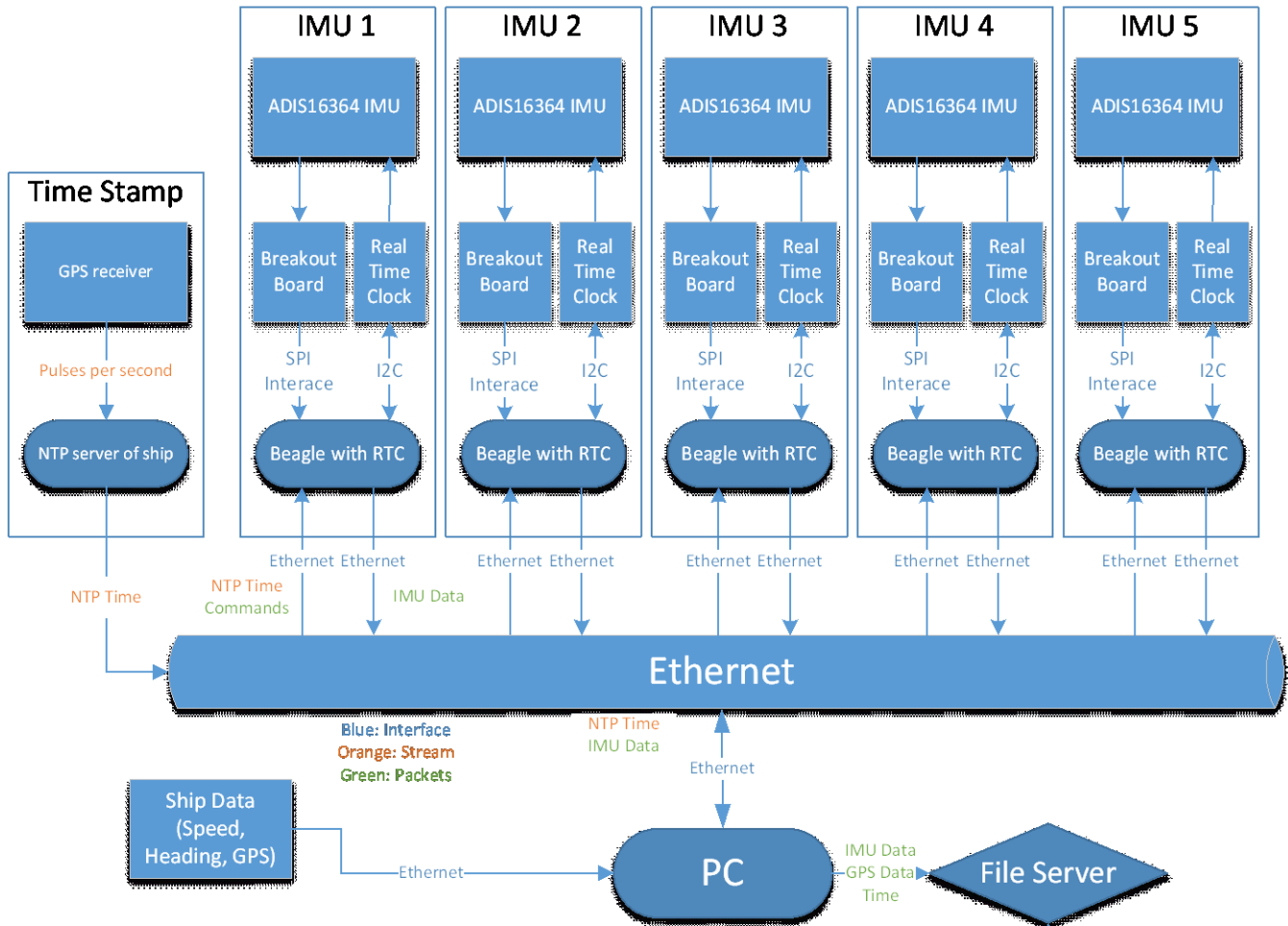


Figure 12. Network structure of distributed inertial sensor setup